Geostatistical Applications to the Estimation of Unconfined and Confined Groundwater Heads in Quasi-3D Groundwater Flow Modeling in Kofu Basin

Xiangwei ZHANG[1], Kuniyoshi TAKEUCHI[2] and Hiroshi ISHIDAIRA[3]

[1]Student Member of JSCE, M. Eng., Graduate School of Civil & Environmental Engineering, Yamanashi University (400-8511 Kofu 4-11-3, Yamanashi, Japan)

[2]Member of JSCE, Ph.D., Professor, Dept. of Civil & Environmental Engineering, Yamanashi University (400-8511 Kofu 4-11-3, Yamanashi, Japan)

[3]Member of JSCE, Dr. of Eng., Associate Professor, Dept. of Civil & Environmental Engineering, Yamanashi University (400-8511 Kofu 4-11-3, Yamanashi, Japan)

When modelling quasi-3D groundwater flow in large area, the spatial distributions of unconfined and confined groundwater heads at each node are necessary. However, the heads of unconfined and confined aquifers are sampled at a limited number of sites whereas values at many un-sampled sites usually are necessary for modeling. On the other hand, the observed heads of the confined aquifer in Kofu basin are less than those of the unconfined aquifer. There is need to incorporate the unconfined head data as auxiliary information into the estimation of the confined head in space. The purpose of this study is to emphasize the supporting role of geostatistics-Residual Ordinary Kriging (ROK) and Universal Cokriging (UCK) in estimating the unconfined and confined heads in space from limited measurements in Kofu basin. Monthly field measurements of the unconfined and confined head in February of 1985 were collected and analyzed using ROK, UCK. The results indicate that accurate results can be obtained by using ROK and UCK.

Key Words: *Unconfined and confined heads, Residual ordinary kriging (ROK), Universal cokriging (UCK)*

1. INTRODUCTION

Numerical simulation of large-scale quasi-3D unsteady groundwater flow often requires initial information of spatial distributions of the unconfined and confined heads. Unfortunately, the heads of unconfined and confined aquifers are sampled at a limited number of sites whereas values at many un-sampled sites usually are needed for modeling. Insufficient observed information decreases the accuracy of modeling calibration and verification, and compromises the quality of quasi-3D groundwater model outputs[1].

In estimating the unconfined and confined head spatial distributions, the major difficulty is to translate measurements at sampled points into space information that reflects spatial distribution of the heads[1), 2)]. In order to overcome such difficulty, geostatistical techniques have been applied to the estimation of the distribution at un-sampled sites[2), 3)]. Since the head in space has a spatial trend, in recent years universal kriging (UK) was often adopted to estimate head distribution with trend[2), 4)]. However, although UK gives a small estimation variance, the dimension of calculation matrix of identifying coefficients is large, and exponentially increases with the order of trend equation [5)]. In order to decrease the dimension of calculation matrix, Neuman[5)] developed Residual Kriging (RK) which separates the measured groundwater head data into drift and residuals, and the residuals alone are put into ordinary kriging (OK). Neuman's work also indicated that RK is simpler than UK, and the resolution of semivariogram is also higher than that of UK.

An important assumption needed for use of OK is that residuals satisfy the stationary condition, i.e. if the distribution of the residual from the trend approximates to normal, the variogram is well estimated, and relatively accurate result can be obtained[7), 11)]. However, the normality of residuals did not consider in RK. Therefore, in this paper, we propose that the trends should be selected in the way that the residuals best fit to the normal distribution and put them into RK algorithm. We propose this method be called as Residual Ordinary Kriging (ROK).

On the other hand, in Kofu basin the measured data of confined heads are less than the unconfined heads.

However, the number of sampled points has a significant influence on the estimated results. Mclaughlin et al.[1] also pointed that the major challenge is to make best use of the limited available information, since subsurface data are difficult and expensive to obtain. Therefore, it is necessary to develop a method to obtain more accurate spatial distribution of confined heads from limited samples in order to make the best use of all available information, particularly, that can be relatively easily obtained. In Kofu basin, the unconfined head may be used as available auxiliary information to estimate confined head.

The purpose of this study is to emphasize the supporting role of two geostatistical approaches—Residual Ordinary Kriging (ROK) and Universal Cokriging (UCK) in estimating spatial distributions of unconfined and confined groundwater heads in Kofu basin. Monthly field measurements of the unconfined and confined head in February of 1985 were collected and analyzed by the two approaches.

Firstly, ROK, in which a polynomial trend was calculated and removed from the original groundwater level data to ensure that the residuals satisfy the stationary condition required for OK, is adopted to estimate the unconfined head. Then the comparison of results between ROK and UK was made.

Secondly, since the water exchange between confined and unconfined aquifers exits, and the unconfined heads are related to the confined heads, UCK is employed to estimate the spatial distribution of confined head using the unconfined heads as auxiliary information.

Finally, to verify the effectiveness of ROK and UCK approaches in estimating the unconfined and confined heads, a case study was carried out in Kofu basin. The results indicate that estimated unconfined and confined heads agree with observed data. Furthermore, the accuracy of results obtained by ROK and UCK is better than that of UK.

2. STUDY AREA

The study area is a part of Kofu basin, where there are unconfined and confined aquifers (**Fig.1**). The unconfined aquifer is formed from deposit with thickness of 15~40 m. In the confined aquifer, the thickness is 10~80 m and the geology is in the finer texture than unconfined aquifer. The clay layer between the unconfined and confined aquifers is semi-pervious with thickness of 0~30 m. Two aquifers are strongly influenced by the geologic structure and the topographic distribution. The elevation ranges from 240 to 1280 m with high elevations in the Southeast and Northwest and low elevation in the West.

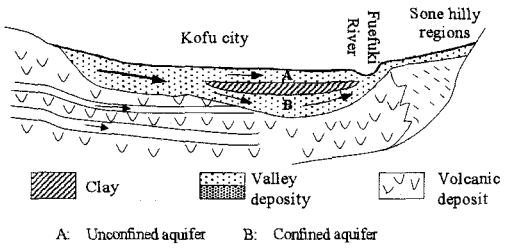

Fig.1 Schematic diagram of geological structure in Kofu basin

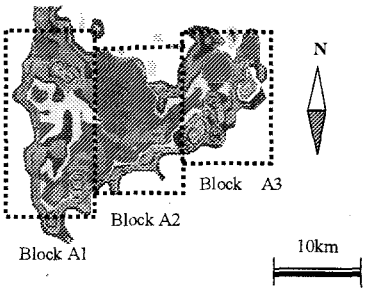

Fig. 2 Distribution maps of soil and rock in Kofu basin

(from KS110-1, Geographical Survey Institute, Japan, 1991)

In the study area, the West and East are mountainous regions with high elevation, and the spatial distribution of soil is heterogeneous. Compared with the West and East, elevation of central part is low, and relatively homogeneous. Thus, on the basis of distribution map of soil, the study area is divided into three blocks A1, A2 and A3 (**Fig.2**).

3. THE ESTIMATION OF UNCONFINED HEAD IN SPACE

(1) Residual ordinary kriging (ROK)

For the spatial distribution of unconfined head, two kinds of spatial variability, i.e. deterministic (trend) and stochastic, have been widely recognized[4), 6), 7)]. Stochastic variability may be further subdivided into spatially dependent and spatially independent variability. Spatial dependence is generally quantified by a variogram, which means that samples spatially closer to each other are more similar than those being farther apart each other. Spatially independent variability includes measurement imprecision, which is usually relatively small, and indistinguishable from measurement. The trend component can be described as a function of position. Hence, the unconfined head $H_1(\mathbf{x})$, that contains trend and spatial components, may be written as[5)]:

$$H_1(\mathbf{x}) = m(\mathbf{x}) + \varepsilon_1(\mathbf{x}) \quad (1)$$

where $\mathbf{x}$ is the position; $m(\mathbf{x})$ is the trend component; $\varepsilon_1(\mathbf{x})$ is the spatially dependent stochastic component.

If distribution of $\varepsilon_1(\mathbf{x})$ is normal, i.e. it satisfies the second-order stationary requirement for OK, $\varepsilon_1(\mathbf{x})$ may be estimated by OK, and then the unconfined head in space can be calculated. Details are as follows:

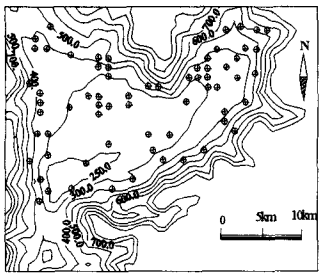

*: The sampled point; —400.0—: Contour of ground

Fig.3 The contour of ground and sampled points for the unconfined head in the study area

a) Calculate trend component $m(\mathbf{x})$, the spatial distribution of unconfined head as a second-order polynomial trend;
b) Remove the trend component from the original unconfined head $H_1(\mathbf{x})$. The residuals, spatially dependent stochastic component $\varepsilon_1(\mathbf{x})$ at sampled sites can be calculated,

$$\varepsilon_1(\mathbf{x}) = H_1(\mathbf{x}) - m(\mathbf{x}) \quad (2)$$

c) The normality is tested for the residuals $\varepsilon_1(\mathbf{x})$ at sampled sites using the Chi-square test. If the normality hypothesis is accepted at the 5% level of significance, $\varepsilon_1(\mathbf{x})$ in the whole study area can be estimated using OK;
d) Finally, substitute trend $m(\mathbf{x})$ and estimated residual $\varepsilon_1(\mathbf{x})$ into Eq.(1), the unconfined heads in the whole study area are then calculated.

(2) Trends and normality test of the residuals in three blocks

There are 66 sampled points of unconfined heads in the study area, as shown in **Fig.3**. The number of sampled points in A1, A2 and A3 are 18, 21 and 27, respectively. Measurements in February of 1985 at 15, 18 and 23 points in A1, A2 and A3 were chosen to calibrate the parameters of ROK. The rest of 10 points, i.e. 3, 3 and 4 sampled points in A1, A2 and A3, respectively, were used as validation samples to assess the validity of the approach.

Fig.3 shows that the elevation drops from east and north to south, which implies a spatial trend in these unconfined heads because of groundwater levels and topography dependence. In general, first and second-order polynomials are chosen as trend equation, they are [9), 10)]:

$$\text{a. } m(\mathbf{x}) = a_0 + a_1 x + a_2 y \quad (3)$$

$$\text{b. } m(\mathbf{x}) = b_0 + b_1 x + b_2 y + b_3 xy + b_4 x^2 + b_5 y^2 \quad (4)$$

where x and y are coordinates.

The selection of the trend equation has a significant effect on normality of the residual. In order to chose a correct trend equation from Eq.(3) and Eq.(4), the residuals $\varepsilon_1(\mathbf{x})$ were calculated, and their normality were tested, respectively.

Table 1 Goodness-of-fit test for residuals

Trend polynomial	Block	Chi-square test		
		χ^2	$\chi^2_{0.05}$	H_0
Eq.(3)	A1	7.331	7.81	A
	A2	4.429	7.81	A
	A3	11.88	7.81	R
Eq.(4)	A1	3.812	7.81	A
	A2	0.895	7.81	A
	A3	1.261	7.81	A

Where χ^2, $\chi^2_{0.05}$ are statistics and the corresponding critical values at the 5% level of significance for Chi-square test. 'A' means that statistic of the Chi-square test is less than the corresponding critical value at the 5% level of significance; therefore the null hypothesis H_0 of normal distribution is accepted, whereas "R" means that H_0 is rejected.

Table 2 The coefficients of Eq.(4)

Block	b_0	b_1	b_2	b_3	b_4	b_5
A1	236.2	0.0137	-0.0009	1.4E-07	-1.7E-06	2.6E-07
A2	258.0	-0.0076	0.0077	-1.1E-06	6.8E-07	4.3E-07
A3	390.4	0.0108	-0.0508	4.1E-07	-1.8E-07	1.6E-06

To test the normality of the residuals in three blocks, Chi-square goodness-of-fit test was employed. The results listed in **Table 1** indicate that the residuals of the observed head from Eq.(3) in A3 do not satisfy the normality assumption through Chi-square test. The reason for the hypothesis H_0 of the normal distribution is rejected can be explained by the fact that the slope of topography changes exponentially, and the ground surface is largely convex in A3. It implies that the trend surface of the residual in block A3 should be a curved surface instead of a plane. As a result, Eq.(3) is not a proper trend equation of the unconfined heads in the block.

On the other hand, for the residuals from Eq.(4), Chi-square goodness-of-fit test gives positive results and the hypothesis H_0 is accepted at the 5% level of significance in all three blocks. **Table 1** also indicates that the means and standard deviations of the residuals from Eq.(4) are less than those of Eq.(3) in all three blocks. Thus Eq.(4) was chosen as trend equation for the three blocks, and their coefficients are listed in **Table 2**.

(3) Estimation of the residuals

Since the spatial distribution of residuals is normal, OK can be used to estimate residuals in the study area.

In this study, three kinds of models, e.g. the Spherical, Exponential and Gaussian models, were employed as theoretical semivariogram models of residuals. For different kind of model, the best-fitted model was selected by using least squares method in Surfer 7.0[8)]. Additionally, in the process of selecting the best-fitted model, there is need of iteration calculation, and the initial value of

Table 3 Parameters of Spherical, Exponential and Gaussian semivariograms for the residuals in three blocks

	Model	AIC	ASD	c_0 (m^2)	c_1 (m^2)	a (km)
Block A1	Gaussian	71.46	4.23	0.05	47.89	5.30
	Spherical	71.42	4.51	0.00	47.11	5.77
	Exponential	71.85	4.75	0.02	49.15	5.01
Block A2	Gaussian	104.76	1.52	0.014	7.82	4.82
	Spherical	106.53	3.50	0.002	8.31	4.38
	Exponential	105.41	2.06	0.00	7.53	4.71
Block A3	Gaussian	78.46	4.34	0.054	19.34	4.61
	Spherical	78.68	4.36	0.00	21.22	4.06
	Exponential	80.86	4.77	0.00	18.76	4.78

the semivariogram range (a) is chosen as the width of block.

In order to determine the best fitted model among three models, the Akaike information criterion (AIC), and minimum average standard deviation (ASD) of the residuals Kriging estimation were adopted[8), 9)].

From **Table 3**, the AIC and ASD for Gaussian model are smallest among three models in Block A2 and Block A3. Meanwhile, although AIC of Gaussian model is larger than that of Spherical model, its ASD is smallest among three models in Block A1. Thus, the Gassian model of Eq.(5) is chosen as best semivariogram model for the residuals in three blocks.

$$\hat{\gamma}(h)=\begin{cases} c_0+c_1(1-\exp(-\frac{h^2}{a^2})), h>0 \\ 0 \qquad\qquad\qquad\qquad h=0 \end{cases} \tag{5}$$

where c_1 is the structural component, which is called as a scale, and a is the correlation range. The coefficients c_0, c_1 and a are listed in **Table 3**.

The variogram range (a) represents the distance beyond which values of the regionalized variable have no longer spatial-correlation. Therefore, from Table 3, a significant spatial-correlation between residuals exists at a range varying from 7.98 km to 9.17 km in three blocks. Since the variogram of unconfined head $h(\mathbf{x})$ is equal to that of the residual $\varepsilon_1(\mathbf{x})$[4), 7)], it implies that the stochastic component of unconfined heads in three blocks also have spatial-correlation within the ranges of 7.98 ~9.17 km, respectively.

(4) Estimated results of unconfined head

On the basis of the estimated residuals in the study area, the unconfined head at each node can be calculated by Eq. (1), and the results are illustrated in **Fig.4**.

In order to compare the accuracy of the estimated unconfined heads using ROK and UK, the differences in the results of ROK and UK in three sections F_1-F_1', F_2-F_2' and F_3-F_3' shown in **Fig.4**, are illustrated in **Fig.5**. It shows that the results of ROK better agree with the measurements than those of UK in sections F_1-F_1' and F_2-F_2',

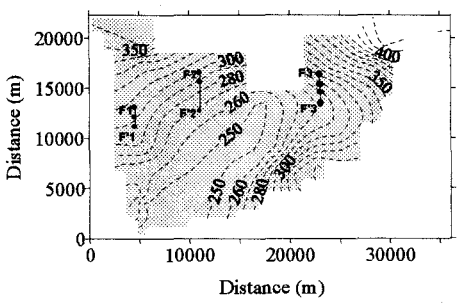

F_1-F_1', F_2-F_2', F_3-F_3' are sections for verifying estimated results

Fig.4 The contour of estimated unconfined head in Kofu basin

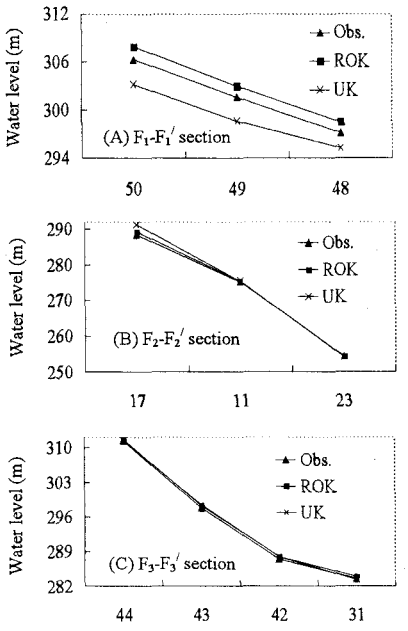

Fig.5 Comparison of the estimated unconfined heads using ROK and UK in three sections

as shown in **Fig.5** (A), (B), and in these two sections where the root-mean-square errors (RMSE) of ROK are 1.46m and 0.53m whereas those of UK are 2.72m and 1.68m, respectively. Obviously, the accuracy of ROK is higher than that of UK in a gentle gradient groundwater surface. For section F_3-F_3', the results of ROK are almost the same as those of UK (**Fig.5** (C)).

4. THE ESTIMATION OF CONFINED HEAD IN SPACE

Since the sampled points of the confined heads are less than those of the unconfined heads in Kofu basin, the observations of confined heads are insufficient. However, if the insufficient information is used to estimate spatial distribution of confined heads, the results of ROK and UK may be unreliable for quasi-3D groundwater numerical simulation.

In order to obtain a relatively accurate spatial estimation of confined head by limited samples, it is necessary to develop a method, which can make the best possible use of available auxiliary information. Although cokriging (CK) for groundwater flow

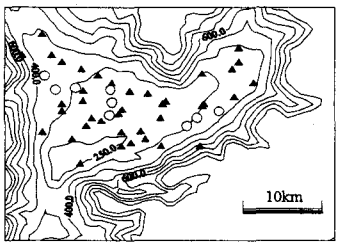

○ The verification point ▲ The sampled point

Fig.6 Sampled points for the confined heads in study area

parameter estimation with auxiliary geophysical data, and UCK for the groundwater surface estimation with auxiliary geological information, have been illustrated in literatures[9), 10)], few studies have embodied unconfined heads as auxiliary information for estimation of confined heads. In this section, therefore, UCK combining the confined heads with the unconfined heads is employed to estimate confined heads in Kofu basin.

(1) UCK embodying the confined and unconfined heads

Considering the confined head H_2 as a primary variable, and the unconfined head H_1 as a secondary variable, cokriging estimate of $\hat{H}_2$ at point $\mathbf{x}_0$ can be written as:

$$\hat{H}_2 = \sum_{i=1}^{n_2} \lambda_i H_{2i} + \sum_{j=1}^{n_1} \omega_j H_{1j} \tag{6}$$

where n_1, n_2 are the numbers of measurement points for H_1, H_2; H_{1j}, H_{2i} are sampled values at point $\mathbf{x}_j, \mathbf{x}_i$; λ_i and ω_j are weights dependent on $H_2(\mathbf{x}_i)$ and $H_1(\mathbf{x}_j)$.

In the case that H_1 and H_2 have spatial trends, H_1 and H_2 would satisfy the following three conditions:

$$\begin{cases} E[H_2(\mathbf{x}+h) - H_2(\mathbf{x})] = m_2(\mathbf{x}) \\ \gamma_2 = \frac{1}{2} E[(H_2(\mathbf{x}+h) - H_2(\mathbf{x}))^2] \end{cases} \tag{7}$$

$$\begin{cases} E[H_1(\mathbf{x}+h) - H_1(\mathbf{x})] = m_1(\mathbf{x}) \\ \gamma_1 = \frac{1}{2} E[(H_1(\mathbf{x}+h) - H_1(\mathbf{x}))^2] \end{cases} \tag{8}$$

$$\gamma_{21} = \frac{1}{2} E[(H_2(\mathbf{x}+h) - H_2(\mathbf{x}))(H_1(\mathbf{x}+h) - H_1(\mathbf{x}))^2] \tag{9}$$

where h is the distance between two points; γ_1, γ_2 and γ_{21} are variograms and cross-variograms for H_1 and H_2; m_1, m_2 are called as drift functions for H_2 and H_1. The following secondary-order drift function is used in this study,

$$m_k(\mathbf{x}) = f_{kl}(x,y) = a_{k,0} + a_{k,1}x + a_{k,2}y + a_{k,3}xy + a_{k,4}x^2 + a_{k,5}y^2 \tag{10}$$

where $a_{k,0} \cdots a_{k,5}$ are coefficients of trend equation; k=H_1 or H_2; $f_{k,0}$=1, $f_{k,1}$=x, $f_{k,2}$=y, $f_{k,3}$=xy, $f_{k,4}$=x^2, $f_{k,5}$=y^2.

The unbiased estimate of $\hat{H}_2$ of Eq.(10), should satisfy $E[\hat{H}_2(\mathbf{x}) - H_2(\mathbf{x})]$=0, so that:

$$E[\sum_{i=1}^{n_2} \lambda_i H_{2i} + \sum_{j=1}^{n_1} \omega_j H_{1j} - H_2(\mathbf{x})] = 0 \tag{11}$$

Table 4 Coefficients of the trend functions for the confined heads in three blocks

Block	A1	A2	A3
$a_{H_2,0}$	228.28	270.16	334.09
$a_{H_2,1}$	-0.0007	-0.0092	0.0049
$a_{H_2,2}$	0.0057	0.0083	-0.0298
$a_{H_2,3}$	-2.51E-07	-9.19E-07	1.07E-06
$a_{H_2,4}$	7.59E-08	6.47E-07	-2.6E-07
$a_{H_2,5}$	8.99E-08	2.50E-07	2.56E-07

Table 5 Parameters of Gaussian functions fitted to experimental variograms for H_2 in three blocks

Parameter	A1	A2	A3
c_1	24.2	10.1	50.5
a	5170	5010	4833

Table 6 Parameters of rational quadric models about cross-variograms for H_1 and H_2 in three blocks

Parameter	A1	A2	A3
c	0.353	4.42	0.892
a	2900	3240	3200

and

$$\begin{cases} \sum_{i=1}^{n_2} \lambda_i f_{H_2,l}(\mathbf{x}_i) = f_{H_2,l}(\mathbf{x}) \\ \sum_{i=1}^{n_1} \omega_j f_{H_1,l}(\mathbf{x}_j) = 0 \end{cases} \quad l = 0,1,\cdots,5 \tag{12}$$

The variance of estimation error is:

$$\sigma_E^2 = Var[\hat{H}_2(\mathbf{x}) - H_2(\mathbf{x})] \tag{13}$$

The objective function (L) is to minimize σ_E^2 with constraint (12), i.e.,

$$L = \sigma_E^2 - 2\sum_{l=0}^{5} \mu_l [\sum_{i=1}^{n_2} \lambda_i f_{H_2,l}(\mathbf{x}_i) - f_{H_2,l}(\mathbf{x})] - 2\sum_{l=0}^{5} \eta_l [\sum_{j=1}^{n_1} \omega_j f_{H_1,l}(x_j)] \tag{14}$$

where μ_l, η_l are lagrange parameters.

Coefficients λ, θ, μ and η can be identified by the minimum of Eq.(14), which is found by setting the partial derivatives of the objective function L to zero.

(2) Estimation of the confined head

On the basis of field monthly measurements of the confined heads at 48 locations in February of 1985 (**Fig.6**), the secondary-order trend functions in three blocks were identified, and their coefficients were listed in **Table 4**. In addition, the trend functions of the unconfined head in three blocks are selected as Eq.(4), and the coefficients are listed in **Table 2**.

a) The fitted variogram models for H_2

The experimental variograms in three blocks for the confined heads can be expressed by the Gaussian model Eq.(5). The parameters of Gaussian functions fitted to experimental variograms were enumerated in **Table 5**.

From **Table 5**, a spatial-correlation for the residuals exists at a range varying from 8.36 to 8.95 km in three blocks. It implies that the confined heads in three

Table 7 A comparison of results using UCK and UK at 9 validation sample points

Point ①	Obs. Value ②	UCK		UK	
		Est. value	Abs. error	Est. value	Abs. error
36	294.70	293.81	0.89	289.92	3.78
37	305.20	304.19	1.01	303.13	2.07
38	320.10	320.50	0.4	321.32	1.22
13	268.50	268.79	0.29	268.88	0.38
14	254.20	254.11	0.08	255.62	1.42
15	249.10	248.74	0.36	250.46	1.36
24	276.00	276.51	0.51	278.39	2.39
26	282.50	282.54	0.04	282.15	0.35
41	300.10	298.18	1.92	297.84	2.26

Where "Obs. Value" means observed value; "Es. Value" means estimated value; "Abs. error" means absolute error.

blocks also have spatial-correlation within the ranges of 8.36－8.95 km, respectively.

b) The fitted cross-variogram models for H_1 and H_2 in three blocks

On the basis of the AIC, it is found that the experimental cross-variogram of γ_{12} and γ_{21} for H_1 and H_2 in block A1 can be expressed by a rational quadric model:

$$r(h) = C\left[\frac{(\frac{h}{a})^2}{1+(\frac{h}{a})^2}\right] \qquad (15)$$

The parameters of Eq.(15) were given in **Table 6**.

c) Estimated results

According to the linear combination of the foregoing fitted models of γ_1, γ_2 and γ_{12}, UCK was performed. The estimated confined heads are shown in **Fig.7**. Because of the relatively high correlation between the unconfined and confined heads, the contours of the confined head are similar in pattern to that of the unconfined head shown in **Fig.4**.

Table 7 shows the estimated results using UCK and UK. It is indicated that since the accuracy of estimated results using geostatistics depends on the given information, relatively accurate results were obtained using UCK owing to the information of the unconfined head being incorporated into estimation process of the confined heads in the UCK. The RMSE of estimated results for 9 sampled points using UCK is 0.85m, which is lower than that of UK's (2.14m).

5. CONCLUSIONS

In this paper, an actual case study for estimating groundwater heads of multi-layer aquifer using spatially correlated field data has been presented based on ROK and UCK approaches. Firstly, the unconfined head spatial distribution was estimated using ROK.

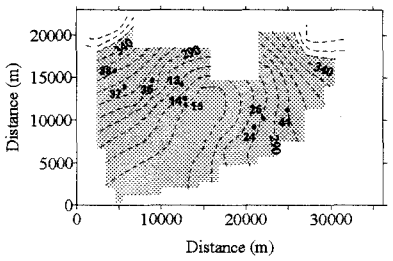

"13,…,38" : Observed points for verifying model

Fig.7 Estimated confined head contour in Kofu Basin using UCK

The advantage of ROK is that matrix dimension of calculation matrix is smaller than that of UK. Furthermore, the results of ROK and UK were compared. It is shown that more accurate results were obtained using ROK.

Secondly, to overcome the difficulty of insufficient measurements of confined head and to increase the accuracy of estimating the spatial distribution of confined head, UCK, which incorporates auxiliary information of the unconfined heads, was employed. Results indicate that the accuracy of UCK estimation is higher than that of UK's.

REFERENCES

1) Mclaughlin, D., Kinzelbach, W. and Ghassemi, F.: Modelling subsurface flow and transport: where do we stand?, Hydrogeologie, No.4, pp.269-280, 1993.
2) Delhomme, J. P.: Kriging in the hydrosciences, Advances in Water Resour., Vol.1, No.5, pp.475-499, 1978.
3) Piggott, A., Bobba, A. G. and Novakowski, K. S.: Regression and inverse analysis in regional groundwater modeling, J. Water Resour. Plan. Manag., Vol. 122, No.1, pp.1-10, 1996.
4) Chen, J. and Wang, H.: Geostatistical Applications to estimate groundwater levels, J. Hydogeo. & Eng. Geo., No. 6, pp.7-11, 1998.
5) Neuman, S.P. and Jacobson, E. A.: Analysis of nonintrinsic spatial variability by residual kriging with application to regional groundwater levels, Mathem. Geo.,, Vol.16, No.5, pp.499-521.
6) Ma, Tain-Shing and M. Sophocleous, and Yu, Yun-Sheng: Geostatistical applications in groundwater modeling in South-Central Kansas, J. Hydrau. Eng., Vol.4, No.1, pp.57-64, 1999.
7) Lamorey, G. and Jacobson, E.: Incorporation of constraints on hydraulic head gradients near no-flow boundary conditions in the determination of spatial drift and their use in an inverse groundwater flow model, Water Resour. Res., Vol.34, No.11, pp.2889-2910, 1998.
8) GSI (Golden Software, Inc.):1999, Surfer-User'S guide.
9) Hamaguchi, T.: Best estimation of cokriging groundwater levels and its cross-correlative effects in using insufficient data set, Annual Journal of Hydraulic Engineering (in Japanese), JSCE, Vol.45, pp.343-348, 2001.
10) Cassiani,G. and Medina, M. A.: Incorporating auxiliary geophysical data into groundwater flow parameter estimation, Ground water, Vol.35, No.2, pp.79-91, 1997

(Received September 30, 2002)